Error estimate of the Non-Intrusive Reduced Basis (NIRB) two-grid method with parabolic equations

August 20, 2022

Elise Grosjean [1], Yvon Maday [2] [3]

Abstract

Reduced Basis Methods (RBMs) are often proposed to approximate solutions of parametric problems. They are useful both to compute solutions for a large number of parameter values (e.g. for parameter fitting) and to approximate a solution for a new parameter value (e.g. real time approximation with a very high accuracy). They aim at reducing the computational costs of High Fidelity (HF) codes. They require well chosen solutions, called snapshots, preliminary computed (e.g. offline) with a HF classical method, involving, e.g. a fine mesh (finite element or finite volume) and generally require a profound modification of the HF code, in order for the online computation to be performed in short (or even real) time.
In this paper, we will focus on the Non-Intrusive Reduced Basis (NIRB) two-grid method. Its main advantage is its efficient way of using the HF code exclusively as a "black-box", unlike other so-called intrusive methods which require a modification of the code. This is very convenient when the HF code is a commercial one and has been purchased, as is often the case in the industry. The effectiveness of this method relies on its decomposition into two stages, one offline (classical in most RBMs as presented above) and one online. The offline part is time-consuming but it is executed only once. On the contrary, the specificity of the NIRB approach is to solve, during the online part, the parametric problem on a coarse mesh only, and then to improve its precision. It is thus much cheaper than a HF evaluation. This method has been initially developed in the context of elliptic equations with finite element and has been extended to finite volume.
In this paper, we generalize the NIRB two-grid method to parabolic equations. To the best of our knowledge, the two-grid method has not already been studied in the context of time-dependent problems. With a model problem, which is the heat equation, we recover optimal estimates in $L^\infty(0,T;H^1(\Omega))$, and present numerical results.

1 Introduction

Let Ω be a bounded domain in $\mathbb{R}^d$, with $d \leq 3$ with smooth enough boundary $\partial\Omega$, and let us consider a parametric problem $\mathcal{P}$ on Ω. Non-Intrusive Reduced Basis (NIRB) methods are an alternative to classical reduced basis methods to approximate the solutions of such problems where the parameter is denoted as μ, in a given set $\mathcal{G}$ [15, 9, 5, 24, 2]. They may be more pratical than intrusive RBMs from an engineering point of view since their uses are simplified by the execution of the HF code only as a "black-box" solver. These methods rely on the assumption that the manifold of all solutions $\mathcal{S} = \{u(\mu), \mu \in \mathcal{G}\}$ has a small Kolmogorov width [20].

Reminders on the NIRB two-grid method for stationnary problems

The two-grid method, in the context of a HF solver of finite element or finite volume type, involves two partitioned meshes (or "grid"), one fine mesh $\mathcal{M}_h$ and one coarse $\mathcal{M}_H$, where the respective sizes h and H of the meshes are such that $h << H$. The size h (respectively H) is defined as

$$h = \max_{K \in \mathcal{M}_h} h_K \text{ (respectively } H = \max_{K \in \mathcal{M}_H} H_K), \tag{1}$$

[1] Felix-Klein-Institut für Mathematik, Kaiserslautern TU, 67657, Deutschland
[2] Sorbonne Université and Université de Paris Cité, CNRS, Laboratoire Jacques-Louis Lions (LJLL), F-75005 Paris, France
[3] Institut Universitaire de France

where the diameter h_K (or H_K) of any element K in a mesh is equal to $\sup_{x,y\in K} |x-y|, K \in M_h$ (or $\in M_H$).

The fine mesh is used for the generation of the Reduced Basis (RB), and the coarse one is used to roughly and rapidly approximate the solution. This coarse mesh and the offline-online decomposition of the algorithm are the key ingredients to the reduction of the complexity. Thus, using the notations for elliptic equations, we carry out the following decomposition:

- First, the RB functions which belong to the reduced space denoted X_h^N are prepared in an "offline" stage with the fine mesh through a greedy procedure or a Proper Orthogonal Decomposition (POD) [23, 3, 12, 6]. The greedy procedure is a way to compute the modes by choosing iteratively some suitable parameters $\mu_1, \ldots, \mu_N \in \mathcal{G}$ and computes the approximate solutions $u_h(\mu_1), \ldots, u_h(\mu_N)$. This part is costly in time, but only executed once, as for other RBMs. At the end of this stage, we obtain N L^2-orthonormalized basis functions, denoted $(\Phi_i^h)_{i=1,..,N}$. At the end of this stage, we obtain N L^2-orthonormalized basis functions, denoted $(\Psi_i^h)_{i=1,\cdots,N}$ after processing a Gram-Schmidt orthonormalization algorithm. In order to enhance the results we may further perform the following eigenvalue problem:

$$\begin{cases} \text{Find } \Phi^h \in X_h^N, \text{ and } \lambda \in \mathbb{R} \text{ such that:} \\ \forall v \in X_h^N, \int_\Omega \nabla \Phi^h \cdot \nabla v \, d\mathbf{x} = \lambda \int_\Omega \Phi^h \cdot v \, d\mathbf{x}, \end{cases} \tag{2}$$

  and we get an increasing sequence of eigenvalues λ_i, and orthogonal eigenfunctions $(\Phi_i^h)_{i=1,\cdots,N}$, orthonormalized in $L^2(\Omega)$ and thus orthogonal in $H^1(\Omega)$, and define a new basis of the space X_h^N.

- Then, for a new parameter μ for which we are interested in estimating the solution, a coarse approximation $u_H(\mu)$ of the solution is first computed "online". This coarse approximation is of course not of sufficient precision but it is calculated much more rapidly compared to the fine mesh one. The NIRB post-processing then makes it possible to notably improve the precision by projection on the RB, within a very short runtime [9, 6, 17, 18, 12]. The classical NIRB approximation is given by

$$u_{Hh}^N(\mu) := \sum_{i=1}^N (u_H(\mu), \Phi_i^h)\ \Phi_i^h.$$

  As proposed in [8], we may also introduce a rectification matrix, denoted $\mathbf{R}$, computed from the coarse snapshots. The latters are generated with the same parameters as for the fine snapshots (during the offline part). Then, we compute the vectors

$$\mathbf{R}_i = (\mathbf{A}^T\mathbf{A} + \delta \mathbf{I}_N)^{-1}\mathbf{A}^T\mathbf{B}_i,\ i = 1, \cdots, N, \tag{3}$$

  where

$$\forall i = 1, \cdots, N, \text{ and } \forall \mu_k \in \mathcal{G},$$

$$A_{k,i} = \int_\Omega \mathbf{u}_H(\mu_k) \cdot \Phi_i^h \, d\mathbf{x}, \tag{4}$$

$$B_{k,i} = \int_\Omega \mathbf{u}_h(\mu_k) \cdot \Phi_i^h \, d\mathbf{x}, \tag{5}$$

  $\mathbf{I}_N$ refers to the identity matrix and δ is a regularization term [9]. The post-treatment applied to NIRB approximation reads

$$Ru_{Hh}^N(\mu) := \sum_{i,j=1}^N R_{ij}\ (u_H(\mu), \Phi_j^h)\ \Phi_i^h,$$

  where $(\cdot,\cdot)$ denotes the L^2-inner product. Note that, up to the relaxation parameter δ the rectification process allows to retrieve the fine coefficients (given in (5)) from the coarse ones (given in (4)) for the parameters $\mu = \mu_k$, $k = 1, .., N$.

Motivation and earlier works. The two-grid method, which can be used for several types of PDEs and approximations, is easy to implement. Moreover, its non-intrusive nature makes it applicable to a wide range of problems. Yet, to the best of our knowledge, this method has not already been studied nor implemented in the context of time-dependent problems [6, 9, 7, 10, 25]. The two-grid method has been developed and analyzed in the context of $\mathbb{P}_1$ FEM (with Céa's and Aubin-Nitsche's lemmas) in [8] for second order elliptic equations. The energy-error estimate then is given by

$$\left\| u(\mu) - u_{Hh}^N(\mu) \right\|_{H^1(\Omega)} \leq \varepsilon(N) + C_1 h + C_2(N) H^2, \tag{6}$$

where C_1 and C_2 are constants independent of h and H, C_2 depends on N, and the term $\varepsilon(N)$ depends on a proper choice of the reduced basis space as a surrogate for the best approximation space associated to the Kolmogorov N-width. It is linked to the error between the fine solution and its projection on X_h^N, given by

$$\left\| u_h(\mu) - \sum_{i=1}^{N} (u_h(\mu), \Phi_i^h)\ \Phi_i^h \right\|_{H^1(\Omega)}. \tag{7}$$

The second term in (6), $C_1\ h$, is a contribution obtained through Céa's lemma for the reduced basis elements and the second one, $C_2(N)\ H^2$, through Aubin-Nitsche's lemma for the coarse grid approximation of $u(\mu)$.
This two-grid method has also been generalized and analyzed in the context of finite volume schemes [12] where a surrogate to Aubin-Nitsche's is used.
This article is about extending NIRB to time-dependent problems and performing its numerical analysis, in the setting of parabolic equations.

Outline of the paper.

We will first theoretically prove that we recover optimal estimates in $L^\infty(0,T;H^1(\Omega))$, and then present numerical results 5. Our main result is given by the theorem 4.1 on the numerical analysis of convergence of the approach. The rest of this paper is organized as follows. In section 2 we describe the mathematical context. In section 3 we present the two-grids method in the context of parabolic equations. Section 4 is devoted to the proof of theorem 4.1. In the last section 5, the implementation is discussed and we illustrate the theoretical results with numerical results on the NIRB method with rectification.

2 Mathematical Background

In the next sections, C will denote various positive constants independent of the size of the meshes h and H and of the parameter μ, and $C(\mu)$ will denote constants independent of the size of the meshes h and H but dependent of μ. We will consider the following heat equation on the domain Ω and with homogeneous Dirichlet conditions, which takes the form

$$\begin{aligned} u_t - \mu\Delta u &= f, \quad \text{in } \Omega\times]0,T[, \\ u(\mathbf{x},0) &= u_0(\mathbf{x}), \quad \text{in } \Omega, \\ u(\mathbf{x},t) &= 0, \quad \text{on } \partial\Omega\times]0,T[, \end{aligned} \tag{8}$$

where $f \in L^2(\Omega\times]0,T[)$, for any $t > 0$, $u(\cdot,t) \in H_0^1(\Omega)$, $u_t \in L^2(\Omega)$ stands for the derivative, $u_0 \in H_0^1(\Omega)$ and $0 < \mu \in \mathcal{G}$ is the parameter. In analogy with the previous work on the NIRB FEM applied to elliptic equations, we consider one fine spatial grid for computing "offline" the snapshots associated with few values of the parameter and one coarse grid for the coarse solution, with sizes respectively denoted as h for the fine mesh and H for the coarse mesh (with $h << H$) (1).These grids are used for the spacial discretizations of the weak formulation of problem (8) while a time stepping method is used to get a fully discrete approximation of the solution of (8). On our model problem, we employed $\mathbb{P}_1$ finite elements for the discretization in space. For the time discretization, we considered finite difference approximation of the time derivative.
We consider two time grids, ending with at time T.

- One time grid, denoted F, is employed for the fine solution (for the snapshots construction). To avoid making notations more cumbersome, we will consider a uniform time grid with Δt_F the interval between two time values. The time levels can be written $t^n = n\ \Delta t_F$, where $n \in \mathbb{N}^*$.

- Another time grid, denoted G, is used for the coarse solution. By analogy with the fine grid, we consider a uniform grid with time step Δt_G. Now, the time levels are written $\widetilde{t}^m = m\ \Delta t_G$, where $m \in \mathbb{N}^*$.

The NIRB algorithm allows us to recover the optimal estimate in space, as in the previous analysis with elliptic equations. There is no such argument as the Aubin-Nitsche's one for time stepping method, hence we need to consider time discretizations that provide the same precision with different time steps hence we consider a higher order time scheme for the coarse solution.
Thus, we deal with three kind of notations:

- $u(\mathbf{x}, t)$ denotes the true solution at time $t \geq 0$ for $\mathbf{x} \in\ \Omega$.
- $u_h(\mathbf{x}, t)$ and $u_H(\mathbf{x}, t)$ that respectively denote the fine and coarse solutions of the spatially semidiscrete solution, at time $t \geq 0$.
- $u_h^n(\mathbf{x})$ and $u_H^m(\mathbf{x})$ that respectively denote the fine and coarse full-discretized solutions at time $t^n = n \times \Delta t_F$ and $\widetilde{t}^m = m \times \Delta t_G$, where Δt_F is the fine time step, and Δt_G is the coarse one.

Remark 2.1. *To simplify the notations, we consider that both time simulations end at time T.*

We use the conventional notations for space-time dependent Sobolev spaces

$$L^p(0,T;V) := \{u(\mathbf{x},t) \mid \|u\|_{L^p(0,T;V)} := \left(\int_0^T \|u(\cdot,t)\|_V^p\ dt\right)^{1/p} < \infty\},\ 1 \leq p < \infty,$$
$$L^\infty(0,T;V) := \{u(\mathbf{x},t) \mid \|u\|_{L^\infty(0,T;V)} := ess \sup_{0\leq t\leq T} \|u(\cdot,t)\|_V < \infty\},\ p = \infty,$$

where V is a real Banach space with norm $\|\cdot\|_V$. The variational form of (8) is given by:

$$\begin{cases} \text{Find } u \in L^2(0,T;H_0^1(\Omega)) \text{ with } u_t \in L^2(0,T;H^{-1}(\Omega)) \text{ such that} \\ (u_t, v) + a(u, v; \mu) = (f, v),\ \forall v \in H_0^1(\Omega) \text{ and } t \in (0,T), \\ u(\cdot, 0) = u_0,\ \text{in } \Omega, \end{cases} \tag{9}$$

where a is given by

$$a(w, v; \mu) = \int_\Omega \mu \nabla w(\mathbf{x}) \cdot \nabla v(\mathbf{x})\ d\mathbf{x}, \quad \forall w, v \in H_0^1(\Omega). \tag{10}$$

We remind that (9) is well posed (see [11] for the existence and the uniqueness of solutions to problem (9)) and we refer to the notations of [11].

Remark 2.2. *(On the stability). We intend to state estimates for the NIRB approximation for all time snapshots n, that is related to maximum-norm in time with the either L^2 norm or H^1 norm in space, ie in $L^\infty(0,T;L^2(\Omega))$ and $L^\infty(0,T;H^1(\Omega))$, which is stronger than with the usual stability study of the parabolic equation* (8)*. Let us remind the classical (or less standard) stability results. We derive from* (9) *by using $v = u$*

$$(u_t, u) + \mu \|\nabla u\|^2 \leq |(f, u)|. \tag{11}$$

From the Young and Poincaré inequalities, there exists $C > 0$ such that

$$|(f,u)| \leq (\frac{C}{2}\|f\|^2) + \frac{\mu}{2}\|\nabla u\|^2.$$

and since

$$(u_t, u) = \frac{1}{2}\frac{d}{dt}\|u\|^2,$$

(11) *yields*

$$\frac{d}{dt}\|u\|^2 + \mu\|\nabla u\|^2 \leq C\|f\|^2,$$

and integrating over $(0,T)$ we end up with

$$\|u(t)\|^2 + \mu \int_0^T \|\nabla u(s)\|^2\ ds \leq C(\|u_0\|^2 + \int_0^T \|f(s)\|^2\ ds),$$

which gives

$$\|u\|^2_{L^\infty(0,T;L^2(\Omega))} + \mu\|u\|^2_{L^2(0,T;H^1_0(\Omega))} \leq C(\|u_0\|^2_{L^2(\Omega)} + \|f\|^2_{L^2(0,T;L^2(\Omega))}).$$

That establishes the first stability result.
For the L^∞ stability in time and H^1 in space, we proceed the same with $v = u_t$ in (9). Integrating over $(0,T)$, it yields

$$\int_0^T \|u_t(s)\|^2 \, ds + \mu \int_0^T \frac{d}{dt}\|\nabla u(s)\|^2 \, ds \leq \int_0^T \|f(s)\|^2 \, ds,$$

which gives

$$\int_0^T \|u_t(s)\|^2 \, ds + \mu\|\nabla u\|^2 \leq \mu \, \|\nabla u_0\|^2 + \int_0^T \|f(s)\|^2 \, ds,$$

and we obtain

$$\|u\|^2_{L^\infty(0,T;H^1_0(\Omega))} \leq \|\nabla u_0\|^2_{L^2(\Omega)} + \frac{1}{\mu}\|f(s)\|^2_{L^2(0,T;L^2(\Omega))},$$

Let V_h and V_H consists of continuous piecewise linear finite element functions which vanish on the boundary $\partial\Omega$. We consider the projection operator P^1_h on V_h (P^1_H on V_H is defined similarly) which is given by

$$(\nabla P^1_h u, \nabla v) = (\nabla u, \nabla v), \quad \forall v \in V_h, \tag{12}$$

The semi-discrete form of the variational problem (9) writes for the fine mesh (similarly for the coarse mesh):

$$\begin{cases} \text{Find } u_h(t) = u_h(\cdot,t) \in V_h \text{ for } t \geq 0 \text{ such that} \\ (\partial_t u_h, v_h) + a(u_h, v_h; \mu) = (f(t^n), v_h), \ \forall v_h \in V_h \text{ and } n \geq 1, \\ u_h(\cdot,0) \ = \ u^0_h \ = \ P^1_h(u^0), \end{cases} \tag{13}$$

The full discrete form of the variational problem (9) for the fine mesh with implicit Euler scheme writes:

$$\begin{cases} \text{Find } u^n_h \in V_h \text{ for } n \geq 0 \text{ such that} \\ (\overline{\partial} u^n_h, v_h) + a(u^n_h, v_h; \mu) = (f(t^n), v_h), \ \forall v_h \in V_h \text{ and } n \geq 1, \\ u_h(\cdot,0) \ = \ u^0_h, \end{cases} \tag{14}$$

where the time derivative in the variational form of the problem (13) has been replaced by a backward difference quotient, $\overline{\partial} u^n_h = \frac{u^n_h - u^{n-1}_h}{\Delta t_F}$,
and with Crank-Nicholson scheme, and $\overline{\partial} u^m_H = \frac{u^m_H - u^{m-1}_H}{\Delta t_G}$, it becomes, for the coarse mesh:

$$\begin{cases} \text{Find } u^m_H \in V_H \text{ for } m \geq 0, \text{ such that} \\ (\overline{\partial} u^m_H, v_H) + a(\frac{u^m_H + u^{m-1}_H}{2}, v_H; \mu) = (f(\widetilde{t^{m-\frac{1}{2}}}), v_H), \ \forall v_H \in V_H \text{ and } m \geq 1, \\ u_H(\cdot,0) \ = \ u^0_H. \end{cases} \tag{15}$$

For $n > 0$, let $\widetilde{u_H}^n$ be a quadratic interpolation in time of the coarse solution at time t^n. We will consider the solutions of (14), and we seek the NIRB approximation with the form

$$\boxed{u^{N,n}_{Hh}(\mathbf{x};\mu) = \sum_{i=1}^N \alpha^H_i(\mu, t^n) \ \Phi^h_i(\mathbf{x}), \ n \geq 0,} \tag{16}$$

where α^H_i are the coarse coefficients and are defined by

$$\alpha^H_i(\mu, t^n) = (\widetilde{u_H}^n(\mu), \Phi^h_i), \tag{17}$$

where $(\Phi^h_i)_{i=1,\ldots,N}$ denotes the L^2 and H^1 orthonormalized basis functions obtained through a greedy procedure (see algorithms 2 or 1 below). Note that they do not depend on time, only the coefficients are time-dependent. This strategy will be detailled in section 3.

Before entering in the proof details of Theorem 4.1, we require a few theorems from [26], on the FEM classical estimates and on both finite difference schemes employed. In the following theorems, we require that the solution of the continuous problem has the regularity implicitly assumed by the presence of the norms on the right. It is well known that with a FEM semi-discretization in space, the following estimate holds.

Theorem 2.3 (Theorem 1.2 [26]). *Let Ω be a convex polyhedron and let u and u_h be the solutions of* (8) *and the semidiscretized variational form* (13)*, respectively. Assume that $u_0 = 0$ on $\partial\Omega$, then*

$$\text{for } t \geq 0, \quad \left\|u(t) - u_h(t)\right\|_{L^2(\Omega)} \leq Ch^2\left[\|u_0\|_{H^2(\Omega)} + \int_0^t \|u_t\|_{H^2(\Omega)}\ ds\right], \tag{18}$$

Once fully discretized on a fine mesh with the backward Euler Galerkin method, the estimate (18) is replaced by the following estimate.

Theorem 2.4 (Theorem 1.5 [26]). *Let Ω be a convex polyhedron and. With u_h^n and u be the solutions of* (14) *and* (8)*, respectively. If $\left\|u_0^h - u_0\right\| \leq Ch^2\|u_0\|_{H^2(\Omega)}$, and $u_0 = 0$ on $\partial\Omega$, we have*

$$\forall n \geq 0 \quad ,\left\|u(t^n) - u_h^n\right\|_{L^2(\Omega)} \leq Ch^2\left[\|u_0\|_{H^2(\Omega)} + \int_0^{t^n} \|u_t\|_{H^2(\Omega)}\ ds\right] + \Delta t_F \int_0^{t^n} \|u_{tt}\|_{L^2(\Omega)}\ ds, \tag{19}$$

With the energy semi-norm, we have the following estimate.

Theorem 2.5 (Theorem 1.4 [26]). *Under the assumptions of Theorem 2.3, we have*

$$\text{for } t \geq 0, \quad \left\|\sqrt{\mu}(\nabla u(t) - \nabla u_h(t))\right\|_{L^2(\Omega)} \leq C(\mu)h\left[\|u_0\|_{H^2(\Omega)} + \left\|u(t)\right\|_{H^2(\Omega)} + (\int_0^t \|u_t\|^2_{H^1(\Omega)}\ ds)^{1/2}\right], \tag{20}$$

where C depends on the parameter μ.

The estimate (20) with the full discretization leads to the following theorem.

Theorem 2.6. *Under the assumptions of Theorem 2.4, we have*

$$\begin{aligned}\forall n \geq 0, \quad \left\|\sqrt{\mu}(\nabla u_h^n - \nabla u(t^n))\right\|_{L^2(\Omega)} \leq & C(\mu)h\left[\|u_0\|_{H^2(\Omega)} + \int_0^{t^n} \|u_t\|_{H^2(\Omega)}\ ds\right] \\ & + \Delta t_F(\int_0^{t^n} \|\nabla u_{tt}\|^2_{L^2(\Omega)}\ ds)^{1/2} + \mathcal{O}(h^2).\end{aligned} \tag{21}$$

Proof. This may be proven by following the same lines as in the proof on the L^2 estimate (Theorem 1.5 [26]), as it is highlighted in [26]. We first decompose the error with two components ρ and θ such that

$$\begin{aligned}\forall n \geq 1,\ e^n := \sqrt{\mu}(\nabla u_h^n - \nabla u(t^n)) &= \sqrt{\mu}((\nabla u_h^n - \nabla P_h^1 u(t^n)) + (\nabla P_h^1 u(t^n) - \nabla u(t^n))) \\ &= \sqrt{\mu}(\nabla\theta^n + \nabla\rho^n).\end{aligned} \tag{22}$$

- For the estimate on ρ, a classical FEM estimate [26, 4] is

$$\left\|P_h^1 v - v\right\|_{L^2(\Omega)} + h\left\|\nabla(P_h^1 v - v)\right\|_{L^2(\Omega)} \leq Ch^2\|v\|_{H^2(\Omega)}, \quad v \in H^2 \cap H_0^1,$$

  which leads to

$$\left\|\nabla\rho^n\right\| \leq Ch\left\|u(t^n)\right\|_{H^2(\Omega)},\ \forall n \geq 0,$$

  and it leads to ,

$$\left\|\nabla\rho^n\right\| \leq Ch\left[\|u_0\|_{H^2(\Omega)} + \int_0^{t^n} \|u_t\|_{H^2(\Omega)}\ ds\right]. \tag{23}$$

- For the estimate on θ, let us consider $v \in V_h$. Since the operators P_h^1 and $\overline{\partial}$ commute, we write

$$(\overline{\partial}\theta^n, v) + \mu(\nabla\theta^n, \nabla v) = (\overline{\partial}u_h^n, v) - (P_h^1\overline{\partial}u(t^n), v) + \mu(\nabla u_h^n, \nabla v) - \mu(\nabla P_h^1 u(t^n), \nabla v).$$

  From (9) and (14), it implies

$$\begin{aligned}(\overline{\partial}\theta^n, v) + \mu(\nabla\theta^n, \nabla v) &= (f, v) - (P_h^1\overline{\partial}u(t^n), v) - \mu(\nabla P_h^1 u(t^n), \nabla v), \\ &= (f, v) - (P_h^1\overline{\partial}u(t^n), v) - \mu(\nabla u(t^n), \nabla v), \text{ by definition of } P_h^1, \\ &= (u_t(t^n), v) - (P_h^1\overline{\partial}u(t^n), v).\end{aligned}$$

Then, with a triangle inequality, it yields

$$\begin{aligned}(\overline{\partial}\theta^n, v) + \mu(\nabla\theta^n, \nabla v) &= -((P_h^1 - I)\overline{\partial}u(t^n), v) + ((\overline{\partial}u(t^n) - u_t(t^n)), v) \\ &:= -(w_1^n + w_2^n, v) = -(w^n, v). \end{aligned} \tag{24}$$

Instead of replacing v by θ^n as in the L^2 estimate, here we replace v by $\overline{\partial}\theta^n$, thus the equation (24) takes the form

$$(\overline{\partial}\theta^n, \overline{\partial}\theta^n) + \mu(\nabla\theta^n, \overline{\partial}\nabla\theta^n) = -(w^n, \overline{\partial}\theta^n).$$

Therefore, by definition of $\overline{\partial}$ for the Backward Euler discretization,

$$\underbrace{(\overline{\partial}\theta^n, \overline{\partial}\theta^n) + \mu\frac{\|\nabla\theta^n\|^2_{L^2(\Omega)}}{\Delta t_F} - \mu\frac{(\nabla\theta^n, \nabla\theta^{n-1})}{\Delta t_F}}_{T_a} = -(w^n, \overline{\partial}\theta^n).$$

With Young's inequality,

$$(\nabla\theta^n, \nabla\theta^{n-1}) \leq \frac{1}{2}\|\nabla\theta^n\|^2_{L^2(\Omega)} + \frac{1}{2}\left\|\nabla\theta^{n-1}\right\|^2_{L^2(\Omega)}.$$

Thus,

$$\left\|\overline{\partial}\theta^n\right\|^2_{L^2(\Omega)} + \mu\frac{\|\nabla\theta^n\|^2_{L^2(\Omega)}}{2\Delta t_F} - \mu\frac{\left\|\nabla\theta^{n-1}\right\|^2_{L^2(\Omega)}}{2\Delta t_F} \leq T_a \leq \frac{1}{2}\|w^n\|^2_{L^2(\Omega)} + \frac{1}{2}\left\|\overline{\partial}\theta^n\right\|^2_{L^2(\Omega)},$$

and it results in

$$\left\|\overline{\partial}\theta^n\right\|^2_{L^2(\Omega)} + \mu\frac{\|\nabla\theta^n\|^2_{L^2(\Omega)}}{\Delta t_F} \leq \mu\frac{\left\|\nabla\theta^{n-1}\right\|^2_{L^2(\Omega)}}{\Delta t_F} + \|w^n\|^2_{L^2(\Omega)}.$$

Since $\left\|\overline{\partial}\theta^n\right\|^2_{L^2(\Omega)} \geq 0$, it follows that

$$\forall n \geq 1,\ \|\nabla\theta^n\|^2_{L^2(\Omega)} \leq \left\|\nabla\theta^{n-1}\right\|^2_{L^2(\Omega)} + \frac{\Delta t_F}{\mu}\|w^n\|^2_{L^2(\Omega)},$$

and we recursively obtain

$$\forall n \geq 1,\ \|\nabla\theta^n\|^2_{L^2(\Omega)} \leq \left\|\nabla\theta^0\right\|^2_{L^2(\Omega)} + \frac{\Delta t_F}{\mu}\sum_{j=1}^{n}\left\|w^j\right\|^2_{L^2(\Omega)}.$$

By definition of θ (and P_h^1),

$$\begin{aligned}\left\|\nabla\theta^0\right\|_{L^2(\Omega)} &= \left\|\nabla u_h^0 - \nabla P_h^1 u(t^0)\right\|_{L^2(\Omega)} \leq \left\|\nabla u_h^0 - \nabla u(t^0)\right\|_{L^2(\Omega)} + \left\|\nabla u(t^0) - P_h^1\nabla u(t^0)\right\|_{L^2(\Omega)} \\ &\leq \left\|\nabla u^0 - \nabla u(t^0)\right\|_{L^2(\Omega)} + Ch\left\|u(t^0)\right\|_{H^2(\Omega)}.\end{aligned}$$

It remains to estimate the L^2 norm of the w^j, defined by (24).

–

$$\begin{aligned}w_1^j &= (P_h^1 - I)\overline{\partial}u(t^j) \\ &= \frac{1}{\Delta t_F}(P_h^1 - I)\int_{t^{j-1}}^{t^j} u_t\, ds, \\ &= \frac{1}{\Delta t_F}\int_{t^{j-1}}^{t^j}(P_h^1 - I)u_t\, ds, \text{ since } P_h^1 \text{ and the time integral commute.}\end{aligned}$$

Thus,

$$\begin{aligned}\frac{\Delta t_F}{\mu}\sum_{j=1}^{n}\left\|w_1^j\right\|^2_{L^2(\Omega)} &\leq \frac{1}{\mu}\sum_{j=1}^{n}\int_{t^{j-1}}^{t^j}\left\|(P_h^1-I)u_t\right\|^2_{L^2(\Omega)}\ ds,\\ &\leq \frac{C}{\mu}h^4\sum_{j=1}^{n}\int_{t^{j-1}}^{t^j}\|u_t\|^2_{H^2(\Omega)}\text{ , by the definition of },P_h^1\\ &\leq \frac{C}{\mu}h^4\int_0^{t^n}\|u_t\|^2_{H^2(\Omega)}\ ds. \end{aligned} \tag{25}$$

– To estimate the L^2 norm of the w_2, we write

$$\begin{aligned} w_2^j &= \frac{1}{\Delta t_F}(u(t^j)-u(t^{j-1}))-u_t(t^j),\\ &= -\frac{1}{\Delta t_F}\int_{t^{j-1}}^{t^j}(s-t^{j-1})u_{tt}(s)\ ds, \end{aligned}$$

such that we end up with

$$\frac{\Delta t_F}{\mu}\sum_{j=1}^{n}\left\|w_2^j\right\|^2_{L^2(\Omega)} \leq \frac{1}{\mu}\sum_{j=1}^{n}\left\|\int_{t^{j-1}}^{t^j}(s-t^{j-1})u_{tt}(s)\ ds\right\|^2_{L^2(\Omega)} \leq \frac{\Delta t_F^2}{\mu}\int_0^{t^n}\|u_{tt}\|^2_{L^2(\Omega)}\ ds.$$

Combining the estimates on ρ and θ concludes the proof.

□

Finally, in the same manner, we can recover the estimate in H^2 and Δt_G^2 with the Crank-Nicolson scheme in the L^2 norm

Theorem 2.7 (Theorem 1.6 [26]). *Let u_H^m be the solution given by* (15)*, associated to Crank-Nicholson discretization with the coarse grids, and u be the solution of* (8)*. Let $\left\|u_0^H-u_0\right\| \leq CH^2\|u_0\|_{H^2(\Omega)}$ and $u_0=0$ on $\partial\Omega$, then*

$$\forall m\geq 0,\quad \left\|u(\widetilde{t}^m)-u_H^m\right\|_{L^2(\Omega)} \leq CH^2\left[\|u_0\|_{H^2(\Omega)}+\int_0^{\widetilde{t}^m}\|u_t\|_{H^2(\Omega)}\ ds\right]+C\Delta t_G^2\int_0^{\widetilde{t}^m}(\|u_{ttt}\|_{L^2(\Omega)}+\|\Delta u_{tt}\|_{L^2(\Omega)})\ ds. \tag{26}$$

3 The Non-Intrusive Reduced Basis method (NIRB) in the context of parabolic equations

3.1 Main steps

This section details the main steps of the two-grids method algorithm in the context of parabolic equations and more precisely how to employ a POD-Greedy algorithm [14, 13, 19] in order to define the reduced basis. Indeed, in the time-discrete formulation, a single solution associated with a parameter μ consists of a sequence of possibly several hundred snapshots over time (each snapshot being a high-fidelity finite element approximation in space at time t^n). Hence, during the greedy algorithm, each greedy step is combined with a temporal compression step performed by a POD. Let us detail the different steps of our offline-online decomposition. The first three points are performed in the offline part, and the others are done online.

1. For each time step n, several fine snapshots $\{\mathbf{u}_h^n(\mu_i)\}_{i\in\{1,...Ntrain\}}$ are computed with the FEM solver, where $\mu_i\in\mathcal{G},\quad \forall i=1,\cdots,Ntrain$.
2. We generate the basis functions (time-independent) $(\Phi_i^h)_{i=1,\cdots,N}$ through a POD-Greedy algorithm as presented in algorithm 1.

In the algorithms 2 and 1, the NIRB L^2 fine projection at each step k is defined by

$$P^{k-1}(\mathbf{u}_h^n(\mu)) = \sum_{i=1}^{k-1} (\mathbf{u}_h^n(\mu), \Phi_i^h)_{L^2}\ \Phi_i^h. \tag{27}$$

and the term

$$\left\| \mathbf{u}_h^n(\mu) - P^{k-1}(\mathbf{u}_h^n(\mu)) \right\|_{L^2} \tag{28}$$

can be calculated either with a set of training snapshots or evaluated with an a-posteriori estimate. Since at each step k, all sets added in the basis are in the orthogonal complement of X_h^{k-1}, it yields an L^2 orthogonal basis without further processing. In practice, the algorithm is halted with a stopping criterion such as an error threshold or a maximum number of basis functions to generate. Then, we solve the following eigenvalue problem:

$$\begin{cases} \text{Find } \Phi_h \in X_h^N, \text{ and } \lambda \in \mathbb{R} \text{ such that:} \\ \forall v \in X_h^N, \int_\Omega \nabla \Phi_h \cdot \nabla v \, d\mathbf{x} = \lambda \int_\Omega \Phi_h \cdot v \, d\mathbf{x}, \end{cases} \tag{29}$$

where $X_h^N = Span\{\Phi_1^h, \ldots, \Phi_N^h\}$. We get an increasing sequence of eigenvalues λ_i, and orthogonal eigenfunctions $(\Phi_i^h)_{i=1,\cdots,N}$, which do not depend on time, orthonormalized in $L^2(\Omega)$ and orthogonalized in $H^1(\Omega)$. Note that with Gram-Schmidt procedure, we only obtain an L^2-orthonormalized RB.

3. For the rectification post-treatment, we generate the equivalent coarse snapshots and the rectification matrix with algorithm 3.

4. We solve the problem (8) on the coarse mesh $\mathcal{T}_H$ for a new parameter $\mu \in \mathcal{G}$ at each time step $m = 0, \ldots, \frac{T}{\Delta t_G}$. Let us denote by $u_H^m(\mu)$ the coarse solution at time $\widetilde{t}^m$. We quadratically interpolate the coarse solution on the fine time grid with the time operator and we obtain n coarse interpolated solutions $\widetilde{u_H}^n(\mu)$.

5. We linearly interpolate $\widetilde{u_H}^n(\mu)$ on the fine mesh in order to compute the L^2-inner product with the basis functions. The approximation used in the two-grid method is

$$\text{For } n = 0, \ldots, \frac{T}{\Delta t_F},\ u_{Hh}^{N,n}(\mu) := \sum_{i=1}^{N} (\widetilde{u_H}^n(\mu), \Phi_i^h)\ \Phi_i^h, \tag{30}$$

and with the rectification post-treatment step [9, 12], it becomes

$$Ru_{Hh}^{N,n}(\mu) := \sum_{i=1}^{N} R_{ij}^n\ (\widetilde{u_H}^n(\mu), \Phi_j^h)\ \Phi_i^h, \tag{31}$$

where R^n is the rectification matrix at time t^n (see algorithm 3).

Algorithm 1 POD-Greedy algorithm used to find $\{\mu_1, n_1, \cdots, \mu_N, n_N\}$

Input: N_{max}, $\{\mathbf{u}_h^n(\mu_1), \cdots, \mathbf{u}_h^n(\mu_{N_{train}})$ with $\mu_i \in \mathcal{G}_{train} \subset \mathcal{G},\ n = 0, \ldots, \frac{T}{\Delta t_F}.\}$
Output: Reduced basis $\{\Phi_1^h, \cdots, \Phi_N^h\}$

Choose $\mu_1, n_1 = \underset{\mu \in \mathcal{G}_{train}, n \in \{0, \ldots, \frac{T}{\Delta t_F}\}}{\arg\max} \left\| \mathbf{u}_h^n(\mu) \right\|_{L^2}$,
$\Phi_1, \cdots, \Phi_{N_1} = POD(\{\mathbf{u}_h^n(\mu_1),\ n = 0, \ldots, \frac{T}{\Delta t_F}.\})$
Set $\mathcal{G}_1 = \mu_1$ and $X_h^1 = \text{span}\{\Phi_1, \cdots, \Phi_{N_1}\}$.
while $\sum_{k=1}^{N} N_k < N_{max}$ **do**
  $\mu_k, n_k = \arg \underset{\mu \in \mathcal{G}_{train},\ n = \{0, \ldots, \frac{T}{\Delta t_F}\}}{\max} \frac{\left\| \mathbf{u}_h^n(\mu) - P^{k-1}(\mathbf{u}_h^n(\mu)) \right\|_{L^2}}{\left\| \mathbf{u}_h^n(\mu) \right\|_{L^2}}$, with P^{k-1} defined by 27.
  $\Phi_{N_{k-1}+1}, \ldots, \Phi_{N_k} = POD(\{\mathbf{u}_h^n(\mu_k) - P^{k-1}(\mathbf{u}_h^n(\mu)),\ n = 0, \ldots, \frac{T}{\Delta t_F}.\})$
  Set $\mathcal{G}_k = \mathcal{G}_{k-1} \cup \mu_k$ and $X_h^k = X_h^{k-1} \oplus \text{span}\{\Phi_{N_1+1}, \cdot, \Phi_{N_k}\}$.
end while

Remark 3.1. *A standard greedy algorithm may also be used but it increases the costs of the offline part. The time is considered as an additional parameter. In the following algorithm, a tolerance treshold is used instead of a priori given number of basis functions.*

Algorithm 2 Greedy algorithm

Input: N_{max}, $\{\mathbf{u}_h^n(\mu_1), \cdots, \mathbf{u}_h^n(\mu_{N_{train}})$ with $\mu_i \in \mathcal{G}_{train} \subset \mathcal{G},\ n = 0, \ldots, \frac{T}{\Delta t_F}.\}$

Output: Reduced basis $\{\Phi_1^h, \cdots, \Phi_N^h\}$

Choose $\mu_1, n_1 = \underset{\mu \in \mathcal{G}_{train},\ n \in \{0,\ldots,\frac{T}{\Delta t_F}\}}{\arg\max} \left\| \mathbf{u}_h^n(\mu) \right\|_{L^2}$,

Set $\Phi_1 = \frac{\mathbf{u}_h^{n_1}(\mu_1)}{\left\| \mathbf{u}_h^{n_1}(\mu_1) \right\|_{L^2}}$

Set $\mathcal{G}_1 = \mu_1, n_1$ and $X_h^1 = \text{span}\{\Phi_1\}$.

for $k = 2$ to N **do**:

$\mu_k, n_k = \arg \underset{\mu \in \mathcal{G}_{train},\ n = \{0,\ldots,\frac{T}{\Delta t_F}\}}{\max} \frac{\left\| \mathbf{u}_h^n(\mu) - P^{k-1}(\mathbf{u}_h^n(\mu)) \right\|_{L^2}}{\left\| \mathbf{u}_h^n(\mu) \right\|_{L^2}}$, with P^{k-1} defined by 27.

Compute $\widetilde{\Phi_k} = \mathbf{u}_h^{n_k}(\mu_k) - \sum_{i=1}^{k-1} (\mathbf{u}_h^n(\mu_k), \Phi_i)_{L^2} \Phi_i$ and set $\Phi_k = \frac{\widetilde{\Phi_k}}{\left\| \widetilde{\Phi_k} \right\|_{L^2}}$

Set $\mathcal{G}_k = \mathcal{G}_{k-1} \cup \mu_k$ and $X_h^k = X_h^{k-1} \oplus \text{span}\{\Phi_k\}$

Stop when $\frac{\left\| \mathbf{u}_h^n(\mu) - P^{k-1}(\mathbf{u}_h^n(\mu)) \right\|_{L^2}}{\left\| \mathbf{u}_h^n(\mu) \right\|_{L^2}} \leq tol\ \forall \mu \in \mathcal{G}_{train},\ \forall n = 0, \ldots, \frac{T}{\Delta t_F}$.

end for

In the offline part, the rectification matrix is computed through the following algorithm

Algorithm 3 algorithm for the offline rectification post-treatment

Input:$\{\mathbf{u}_h^n(\mu_1), \cdots, \mathbf{u}_h^n(\mu_{N_{train}})$, with $\mu_i \in \mathcal{G}_{train} \subset \mathcal{G},\ n = 0, \ldots, \frac{T}{\Delta t_F}.\}$ and with the same parameter $\{\mathbf{u}_H^m(\mu_1), \cdots, \mathbf{u}_H^m(\mu_{N_{train}})$, with $\mu_i \in \mathcal{G}_{train} \subset \mathcal{G},\ m = 0, \ldots, \frac{T}{\Delta t_G}.\}$

Output: Rectification matrix $R_{i,j}^n,\ n = 0, \ldots, \frac{T}{\Delta t_F}$.

Realize the quadratic interpolation of the coarse snapshots in time, denoted $\widetilde{\mathbf{u}_H}^n,\ n = 0, \ldots, \frac{T}{\Delta t_F}$.

for $n = 0, \ldots, \frac{T}{\Delta t_F}$: **do**

Calculate the fine and coarse coefficients

$\forall i = 1, \cdots, N$, and $\forall \mu_k \in \mathcal{G},\ A_{k,i}^n = \int_\Omega \widetilde{\mathbf{u}_H}^n(\mu_k), \cdot, \Phi_i^h\ d\mathbf{x}$, and $B_{k,i}^n = \int_\Omega \mathbf{u}_h^n(\mu_k) \cdot \Phi_i^h\ d\mathbf{x}$,

For $i = 1, \cdots, N$, set $\mathbf{R}_i^n = (\mathbf{A^n}^T \mathbf{A^n} + \delta \mathbf{I}_N)^{-1} \mathbf{A^n}^T \mathbf{B^n}_i$.

end for

In the subsequent section, we demonstrate the optimal error in $L^\infty(0, T; H^1(\Omega))$.

4 NIRB error estimate with parabolic equations

Main result Our main result is concerned with the following theorem.

Theorem 4.1. *NIRB error estimate for parabolic equations. Let us consider the problem 8 and its exact solution $u(\boldsymbol{x}, t; \mu)$, and the full discretized solution to the problem 14. Let $(\Phi_i^h)_{i=1,\ldots,N}$ be the L^2-orthonormalized and H^1-orthogonalized RB generated with the POD-greedy algorithm 1 from the fine solutions of (14), on a fine mesh of size h, with $\mathbb{P}_1$ FE for the spatial discretization, and a Backward Euler scheme for the time discretization. For $m = 0, \ldots, \frac{T}{\Delta t_G}$, let $u_H^m(\mu)$ be the coarse approximation of (14) for $\mu \in \mathcal{G}$, on a coarse mesh of size H, with a $\mathbb{P}_1$ FEM for the spatial discretization, and a Crank-Nicolson scheme for the time discretization.*

Let us consider the NIRB approximation, defined by (16) *and derived from these solutions. Then, the following estimate holds*

$$\text{for } n = 0, \dots, \frac{T}{\Delta t_F}, \left\| u(t^n)(\mu) - u_{Hh}^{N,n}(\mu) \right\|_{H^1(\Omega)} \leq \varepsilon(N) + C_1(\mu)h + C_2(N)H^2 + C_3(\mu)\Delta t_F + C_4(N)\Delta t_G^2, \tag{32}$$

where C_1, C_2, C_3 and C_4 are constants independent of h and H, Δt_F and Δt_G. The term ε depends on the Kolmogorov N-width and measures the error given by (7)*. If H is such as $H^2 \sim h$, $\Delta t_G^2 \sim \Delta t_F$, and $\varepsilon(N)$ is small enough, it results in an error estimate in $\mathcal{O}(h + \Delta t_F)$.*

Theorem 4.1 proves that the NIRB two grids method can be applied to parabolic problems. We recover optimal error estimates in $L^\infty(0, T; H^1(\Omega))$. We emphasize that the choice of the finite difference scheme is motivated by the fact that we want the coarse solution to be coarser in space as well as in time, compared to the fine solution.

Remark 4.2. *This theorem can be generalized to $\mathbb{P}_k$ FEM space, with $k > 1$.*

With the L^2 norm, we obtain the following theorem.

Theorem 4.3. *With the same assumptions than theorem 4.1, with the L^2 orthonormalized RB, the following estimate holds*

$$\text{for } n = 0, \dots, \frac{\Delta t_F}{T}, \left\| u(t^n)(\mu) - u_{Hh}^{N,n}(\mu) \right\|_{L^2(\Omega)} \leq \varepsilon'(N) + C_1'(H^2 + \Delta t_G^2) + C_2'(h^2 + \Delta t_F), \tag{33}$$

where C_1' and C_2' are constants independent of h, H and N, and ε' depends on the Kolmogorov N-width, and corresponds to the L^2 error between the fine solution and its projection on the reduced space.

We now go on with the proof of Theorem 4.1.

Proof. The NIRB approximation at time step $n = 0, \dots, \frac{T}{\Delta t_F}$, for a new parameter $\mu \in \mathcal{G}$ is defined by (16). Thus, the triangle inequality gives

$$\forall t = n \times \Delta t_F, \tag{34}$$

$$\begin{aligned} \left\| u(t)(\mu) - u_{Hh}^{N,n}(\mu) \right\|_{H^1(\Omega)} &\leq \left\| u(t)(\mu) - u_h^n(\mu) \right\|_{H^1(\Omega)} + \left\| u_h^n(\mu) - u_{hh}^{N,n}(\mu) \right\|_{H^1(\Omega)} + \left\| u_{hh}^{N,n}(\mu) - u_{Hh}^{N,n}(\mu) \right\|_{H^1(\Omega)} \\ &=: T_1 + T_2 + T_3, \end{aligned} \tag{35}$$

where $u_{hh}^{N,n}(\mu) = \sum_{i=1}^{N} (u_h^n(\mu), \Phi_i^h)\ \Phi_i^h$.

- The first term T_1 may be estimated using the inequality (21), such that

$$\left\| u(t)(\mu) - u_h^n(\mu) \right\|_{H^1(\Omega)} \leq C(\mu)\ (h + \Delta t_F). \tag{36}$$

- We denote by $\mathcal{S}_h = \{u_h(\mu, t), \mu \in \mathcal{G}, t \in [0, T]\}$ the set of all the solutions. For our problem model, this manifold has a low complexity. It means that for an accuracy $\varepsilon = \varepsilon(N)$ related to the Kolmogorov N-width of the manifold $\mathcal{S}_h$, for any $\mu \in \mathcal{G}$, and any $n \in 0, \dots, \frac{T}{\Delta t_F}$, T_2 is bounded by ε which depends on the Kolmogorov N-width.

$$T_2 = \left\| u_h^n(\mu) - \sum_{i=1}^{N} (u_H^n(\mu), \Phi_i^h)\ \Phi_i^h \right\|_{H^1(\Omega)} \leq \varepsilon(N). \tag{37}$$

- The third term T_3 depends on the method used to create the RB.

1. Let us first consider the greedy approach with a Gram-Schmidt procedure and an eigenvalue problem (29), which yields to an orthogonalization in L^2 and in H_1. Therefore,

$$\left\| u_{hh}^{N,n} - u_{Hh}^{N,n} \right\|_{H^1(\Omega)}^2 = \sum_{i=1}^{N} |(u_h^n(\mu) - \widetilde{u_H}^n(\mu), \Phi_i^h)|^2 \left\| \Phi_i^h \right\|_{H^1(\Omega)}^2, \tag{38}$$

where $\widetilde{u_H}^n(\mu) = U_{H,2}(t^n; \mu)$ is a continuous and piecewise quadratic reconstruction of our coarse solution at time t^n, $\forall n = 0, \dots, \frac{T}{\Delta t_F}$, defined as in [1]. Indeed, we want to recover the second order

in time of the Crank-Nicolson scheme and a linear reconstruction in time leads to suboptimal bounds [22]. To simplified the notations, we introduce $u_H^{n-\frac{1}{2}} = \frac{1}{2}(u_H^n + u_H^{n-1})$. To construct such quadratic reconstruction, let us first consider $U_{H,1}$ the linear reconstruction of u_H^m in $I_m = (I_{m-1}, I_m]$ given by

$$U_{H,1}(t,\mathbf{x}) := u_H^{m-\frac{1}{2}}(\mathbf{x}) + (t - \widetilde{t}^{m-\frac{1}{2}})\ \overline{\partial} u_H^m(\mathbf{x}),\ t \in I_m,\ m = 1,\dots,\frac{T}{\Delta t_G},\ \mathbf{x} \in \Omega. \tag{39}$$

with $U_{H,1}(0) = u_H^0$. Then, we define the continuous and piecewise quadratic function $U_{H,2} : [0,T] \times \Omega \to V_h$ of the approximate solution u_H^m, $m = 0,\dots,\frac{T}{\Delta t_G}$ as

$$U_{H,2}(t,\mathbf{x}) := u_H^{m-1}(\mathbf{x}) - \int_{\widetilde{t}^{m-1}}^{t} [\mu \Delta U_{H,1}(s,\mathbf{x})]\ ds + \Psi(t), \forall t \in (\widetilde{t}^{m-1}, \widetilde{t}^m],\ m = 1,\dots,\frac{T}{\Delta t_G},\ \text{and } \forall \mathbf{x} \in \Omega, \tag{40}$$

where $\Psi(t)$ is a piecewise quadratic polynomial given by

$$\Psi(t) = (t - \widetilde{t}^{m-1}) f(\widetilde{t}^{m-\frac{1}{2}}) - \frac{1}{\Delta t_G}(t - \widetilde{t}^{m-1})(\widetilde{t}^m - t)[f(\widetilde{t}^{m-\frac{1}{2}}) - f(\widetilde{t}^{m-1})],\ \forall t \in I_m. \tag{41}$$

From the RB orthonormalization in L_2, the equation (29) yields

$$\left\|\Phi_i^h\right\|_{H^1}^2 := \left\|\nabla \Phi_i^h\right\|_{L^2(\Omega)}^2 = \lambda_i \left\|\Phi_i^h\right\|_{L^2(\Omega)}^2 = \lambda_i \leq \max_{i=1,\cdots,N} \lambda_i = \lambda_N, \tag{42}$$

such that the equation (38) yields

$$\left\|u_{hh}^{N,n} - u_{Hh}^{N,n}\right\|_{H^1(\Omega)}^2 \leq C\lambda_N \left\|u_h^n(\mu) - \widetilde{u_H}^n(\mu)\right\|_{L^2(\Omega)}^2. \tag{43}$$

From [1], with some adjustments (here we consider fully discrete approximate solutions, and A is replaced by a laplacian), we know that

Proposition 4.4. *with $U_{H,1}$ and $U_{H,2}$ defined by* (39) *and* (40) *respectively,*

$$\max_{t \in I_n} |u_H^2(t,\boldsymbol{x}) - u_H^1(t,\boldsymbol{x})| \leq \mathcal{O}(\Delta t_G^2),\ \forall \boldsymbol{x} \in \Omega. \tag{44}$$

Proof. We introduce a discrete Laplacian $\Delta_H : V_H \to V_H$ by

$$(\Delta_H \psi, \xi) = (\nabla \psi, \nabla \xi),\ \forall \psi, \xi \in V_H.$$

With this notation the semidiscrete equation (in space) takes the form

$$(\partial_t u_H(t), v_H) + \mu(\Delta_H u_H(t), v_H) = (P_H^0 f(t), v_H),\ \forall v_H \in V_H,\ t > 0, \tag{45}$$

where the orthogonal projection of V onto V_H with respect to the inner product in L^2 is denoted P_H^0. Since all the factors on the left are in V_h, (45) may be written as

$$\partial_t u_H(t) + \mu \Delta_H u_H(t) = P_H^0\ f(t),\ t > 0,\ \text{with } u_H(0) = u_H^0. \tag{46}$$

Then $\Delta_H P_H^1 = P_H^0 \Delta$, and we have

$$(\Delta_H P_H^1 v,\ \xi) = -(\nabla P_H^1 v, \nabla \xi) = -(\nabla v, \nabla \xi) = (\Delta v, \xi) = (P_H^0 \Delta v, \xi),\ \forall v \in V,\ \xi \in V_H,$$

thus, we will henceforth stick to the unique notation Δ, meaning the Laplacian on $H_0^1(\Omega)$ and the discrete Laplacian on V_H.
Evaluating the integral in (40) by the trapezoidal rule, we have

$$\begin{aligned} &\forall t \in (\widetilde{t}^{m-1}, \widetilde{t}^m],\ m = 1,\dots,\frac{T}{\Delta t_G},\ \text{and } \forall \mathbf{x} \in \Omega, \\ &U_{H,2}(t,\mathbf{x}) := u_H^{m-1}(\mathbf{x}) - \frac{1}{2}(t - \widetilde{t}^{m-1})[\mu \Delta U_{H,1}(t,\mathbf{x}) + \mu \Delta u_H^{m-1}(\mathbf{x})] + \Psi(t). \end{aligned} \tag{47}$$

We have $U_{H,2}(\widetilde{t}^{m-1},\mathbf{x}) = u_H^{m-1}(\mathbf{x})$, and $u_{H,2}(\widetilde{t}^{m},\mathbf{x}) = u_H^{m-1}(\mathbf{x}) - \Delta t_G \mu \Delta u_H^{m-\frac{1}{2}}(\mathbf{x}) + \Delta t_G f(\widetilde{t}^{m-\frac{1}{2}}) = u_H^m(\mathbf{x})$, from (15) and since v_h in the weak formulation is arbitrary.
Then,

$$\int_\Omega |U_{H,2}(t,\mathbf{x}) - U_{H,1}(t,\mathbf{x})|^2 = \int_\Omega |u_H^{m-1}(\mathbf{x}) - U_{H,1}(t,\mathbf{x}) - \frac{1}{2}(t-\widetilde{t}^{m-1})\mu[\Delta U_{H,1}(t,\mathbf{x}) + \Delta u_H^{m-1}(\mathbf{x})] + \Psi(t)|^2. \tag{48}$$

and since

$$\begin{aligned} u_H^{m-1}(\mathbf{x}) - U_{H,1}(t,\mathbf{x}) &= u_H^{m-1}(\mathbf{x}) - \frac{1}{2}(u_H^m(\mathbf{x}) + u_H^{m-1}(\mathbf{x})) - (t-\widetilde{t}^{m-\frac{1}{2}}\frac{1}{\Delta t_G}(u_H^m - u^{m-1}), \\ &= -(t-\widetilde{t}^{m-1})\frac{u_H^m(\mathbf{x}) - u_H^{m-1}(\mathbf{x})}{\Delta t_G}, \end{aligned}$$

equation (48) becomes

$$\int_\Omega |U_{H,2}(t,\mathbf{x}) - U_{H,1}(t,\mathbf{x})|^2 = \int_\Omega | -(t-\widetilde{t}^{m-1})\frac{u_H^m(\mathbf{x}) - u_H^{m-1}(\mathbf{x})}{\Delta t_G} - \frac{1}{2}(t-\widetilde{t}^{m-1})\mu[\Delta U_{H,1}(t,\mathbf{x}) + \Delta u_H^{m-1}(\mathbf{x})] + \Psi(t)|^2.$$

and from (15) it yields

$$\begin{aligned} \int_\Omega |U_{H,2}(t,\mathbf{x}) - U_{H,1}(t,\mathbf{x})|^2 &= \int_\Omega |(t-\widetilde{t}^{m-1})[\mu\Delta u_H^{m-\frac{1}{2}} - f(t^{n-\frac{1}{2}})] - \frac{1}{2}(t-\widetilde{t}^{m-1})\mu[\Delta U_{H,1}(t,\mathbf{x}) + \Delta u_H^{m-1}(\mathbf{x})] + \Psi(t)|^2, \\ &= \int_\Omega | -\frac{1}{2}(t-\widetilde{t}^{m-1})[\mu\Delta U_{H,1}(t,\mathbf{x}) - \mu\Delta u_H^m(\mathbf{x})] + \Psi(t) - (t-\widetilde{t}^{m-1})f(t^{n-\frac{1}{2}})|^2. \end{aligned}$$

By definition of Ψ (41), we end up with

$$\int_\Omega |U_{H,2}(t,\mathbf{x}) - U_{H,1}(t,\mathbf{x})|^2 = \int_\Omega |(t-\widetilde{t}^{m-1})(\widetilde{t}^{m}-t)[\frac{1}{2}\mu\Delta(\frac{u_H^m - u_H^{m-1}}{\Delta t_G}) - \frac{1}{\Delta t_G}[f(t^{n-\frac{1}{2}}) - f(t^{n-1})]|^2. \tag{49}$$

which is in $\mathcal{O}(\Delta t_G^4)$. □

We now resume the proof of 4.1.
For $m \in 1,\dots\frac{T}{\Delta t_G}$, let $\widetilde{t}^{m-1} \in (t^{n-1},t^n]$, then $t^n \in I_m$, and we now that for $t^n \in I_m$,

$$U_{H,1}(t^n) = u_H^{m-1} + (t^n - \widetilde{t}^{m-1})\frac{u_H^m - u_H^{m-1}}{\Delta t_G}.$$

By definition of $U_{H,1}$ and from the triangle inequality and theorems 2.4 and 26, for $t^n \in I_m$,

$$\begin{aligned} \left\|U_{H,1}(t^n) - u_h^n\right\|_{L^2(\Omega)} &= \left\| u_h^n - u_H^{m-1} - (t^n - \widetilde{t}^{m-1})\frac{u_H^m - u_H^{m-1}}{\Delta t_G} \right\|_{L^2(\Omega)}, \\ &\leq \left\|u_h^n - u_h(t^n)\right\|_{L^2(\Omega)} + \left\| u_h(t^n) - u_H^{m-1} - (t^n - \widetilde{t}^{m-1})\frac{u_H^m - u_H^{m-1}}{\Delta t_G} \right\|_{L^2(\Omega)}, \\ &\leq C(H^2 + \Delta t_F), \text{ since } t^n - \widetilde{t}^{m-1} \text{ is in } \mathcal{O}(\Delta t_F). \end{aligned} \tag{50}$$

Combining (49)-(50), it yields

$$\left\|u_h^n(\mu) - \widetilde{u_H}^n(\mu)\right\|_{L^2(\Omega)}^2 \leq C(H^4 + \Delta t_G^4). \tag{51}$$

By theorem 26 and the triangle inequality, we end up for equation (43) with

$$\left\|u_{hh}^{N,n} - u_{Hh}^{N,n}\right\|_{H^1(\Omega)} \leq C\sqrt{\lambda_N}(H^2 + \Delta t_G^2), \tag{52}$$

where C does not depend on N. Combining these estimates (36), (37) and (52), we obtain the estimate (32).

2. Now we consider only an L^2-orthonormalized basis, which we will denote $(\Psi_{h,i})_{i=1,\dots,N}$ (obtained by a Gram-Schmidt algorithm or with the Greedy-POD algorithm 1). The functions $(\Psi_{h,i})_{i=1,\dots,N}$ and $(\Phi_i^h)_{i=1,\dots,N}$ are both generators of X_h^N. Thus, there exists $(\gamma^i)_{i=1,\dots,N} \in \mathbb{R}^N$ such that $\Psi_{h,i} = \sum_{j=1}^{N} \gamma_j^i \Phi_i^h$. By the H^1-orthogonality of the $(\Phi_i^h)_{j=1,\dots,N}$, it follows

$$\begin{aligned}
\left\|\Psi_{h,i}\right\|_{H^1}^2 &= \sum_{j=1}^{N} |\gamma_j^i|^2 \left\|\Phi_i^h\right\|_{H^1}^2, \\
&\leq \lambda_N \sum_{j=1}^{N} |\gamma_j^i|^2 \left\|\Phi_i^h\right\|_{L^2(\Omega)}^2 \text{ by equation (29)}, \\
&= \lambda_N \left\|\Psi_{h,i}\right\|_{L^2(\Omega)}^2 \text{ by the } L^2\text{-orthogonality of the } (\Psi_{h,i}^n)_{i=1,\dots,N}. \qquad (53)
\end{aligned}$$

From the estimate (53) and the L_2-orthonormalization of the RB,

$$\begin{aligned}
\left\|u_{hh}^{N,n}(\mu) - u_{Hh}^{N,n}(\mu)\right\|_{H^1} &\leq \sum_{i=1}^{N} |(u_h^n(\mu) - \widetilde{u_H}^n(\mu), \Psi_{h,i}^n)| \left\|\Psi_{h,i}\right\|_{H^1}, \\
&\leq C\sqrt{\lambda_N} \sum_{i=1}^{N} |(u_h^n(\mu) - \widetilde{u_H}^n(\mu), \Psi_{h,i})|. \qquad (54)
\end{aligned}$$

From Cauchy-Schwarz inequality, inequality (54) leads to

$$\begin{aligned}
\left\|u_{hh}^{N,n}(\mu) - u_{Hh}^{N,n}(\mu)\right\|_{H^1} &\leq C\sqrt{\lambda_N}\sqrt{N} \sqrt{\sum_{i=1}^{N} |(u_h^n(\mu) - \widetilde{u_H}^n(\mu), \Psi_{h,i})|^2}, \\
&\leq C\sqrt{\lambda_N}\sqrt{N} \left\|u_h^n(\mu) - \widetilde{u_H}^n(\mu)\right\|_{L^2(\Omega)}.
\end{aligned}$$

From the estimate 51, we end up with

$$\left\|u_{hh}^{N,n}(\mu) - u_{Hh}^{N,n}(\mu)\right\|_{H^1} \leq C\sqrt{N}\sqrt{\lambda_N}(H^2 + \Delta t_G^2), \qquad (55)$$

which leads to estimate (32) using the inequalities (36), (37), and (55), and concludes the proof.

□

Therefore, with an L^2 and H^1 orthogonalized RB, the constant C_2 in theorem 4.1 has a smaller dependence regarding the number of modes N. Thus, the NIRB approximation is stabilized with the H^1 orthogonality, compared with a RB only orthogonalized in L^2.

L^2 estimate. We proceed with the proof of theorem 4.3.

Proof. In analogy with the H^1 estimate, we have

$$\begin{aligned}
\forall n = 0, \dots, \frac{T}{\Delta t_F}, \left\|u(t^n)(\mu) - u_{Hh}^{N,n}(\mu)\right\|_{L^2} &\leq \left\|u(t^n)(\mu) - u_h^n(\mu)\right\|_{L^2} + \left\|u_h^n(\mu) - u_{hh}^{N,n}(\mu)\right\|_{L^2} + \left\|u_{hh}^{N,n}(\mu) - u_{Hh}^{N,n}(\mu)\right\|_{L^2} \\
&=: T_1 + T_2 + T_3. \qquad (56)
\end{aligned}$$

- For the first term T_1, it follows theorem 2.4 that

$$T_1 \leq C(h^2 + \Delta t_F). \qquad (57)$$

- As with the H^1 estimate, T_2 can be estimated with the Kolmogorov N-width, and thus, for an accuracy $\varepsilon' = \varepsilon'(N) \leq \varepsilon(N)$,

$$T_2 \leq \varepsilon'. \qquad (58)$$

- For the last term T_3, by L^2-orthonormality,

$$\left\|u_{hh}^{N,n}(\mu) - u_{Hh}^{N,n}(\mu)\right\|_{L^2(\Omega)}^2 = \sum_{i=1}^{N} |(u_h^n(\mu) - u_H^n(\mu), \Psi_{h,i}^n)|^2 \left\|\Phi_i^h S\right\|_{L^2(\Omega)}^2, \\ \leq C \left\|u_h^n(\mu) - u_H^n(\mu)\right\|_{L^2(\Omega)^2}. \tag{59}$$

  By theorem 26 and triangle inequality, it leads to

$$\left\|u_{hh}^{N,n}(\mu) - u_{Hh}^{N,n}(\mu)\right\|_{L^2(\Omega)}^2 \leq C\ (H^2 + \Delta t_G^2). \tag{60}$$

  Combining (56) with (57), (58), (60) concludes the proof.

□

5 Numerical results.

In this section, we applied the NIRB algorithm on several numerical tests:

- First, on the model problem with $\Delta t_G = \frac{\Delta t_F}{2}$. Note that in some situations, because of the constant C_4 in the estimate of theorem 4.1, the best size for the coarse mesh may not be $\Delta t_F^{1/2}$.
- Then, on the model problem with $\Delta t_G^2 = \Delta t_F$. In this test, we use finer grids.
- Finally, we also test our problem on a more complex problem, which is the Brusselator equations. In this case, we use RK2 for the coarse time scheme.

5.1 $\Delta t_G = \frac{\Delta t_F}{2}$

With the following notation

$$F(t) = \mu \Delta u(t) + f(t),$$

the Backward Euler scheme writes

$$\frac{u^{n+1} - u^n}{\Delta t_F} = F^{n+1},$$

which, with a test function $v \in H_0^1(\Omega)$, gives in its weak formulation

$$(u^{n+1}, v) + \ \Delta t_F\ \mu(\nabla u^{n+1}, \nabla v)\ =\ \Delta t_F (f^{n+1}, v) + (u^n, v), \tag{61}$$

whereas the Crank-Nicholson is defined by

$$\frac{u^{n+1} - u^n}{\Delta t_G} = \frac{1}{2}(F^{n+1} + F^n),$$

and the corresponding variational formulation reads

$$(u^{n+1}, v) + \frac{1}{2}\Delta t_G\ \mu(\nabla u^{n+1}, \nabla u^n)\ =\ \frac{1}{2}\Delta t_G((f^{n+1} + f^n, v)\ -\ \mu(\nabla u^n, \nabla v)) + (u^n, v). \tag{62}$$

We tested the two-grid method with the rectification post-treatment 3 on the problem (8) with $\mathcal{G} = (0, 10]$ and the right-hand side function

$$f(t, \mathbf{x}) = 10[x^2(x-1)^2 y^2(y-1)^2 - 2t((6x^2 - 6x + 1)(y^2(y-1)^2) + (6y^2 - 6y + 1)(x^2(x-1)^2))],$$

where $\mathbf{x} = (x, y)$. The rectification post-processing step is done for each time step. Thus the NIRB with rectification is given by

$$Ru_{Hh}^{N,n}(\mu) = \sum_{i,j=1}^{N} R_{ij}^n\ \alpha_j^H(\mu, t^n)\ \Phi_i^h(\mathbf{x}),\ n \geq 0, \tag{63}$$

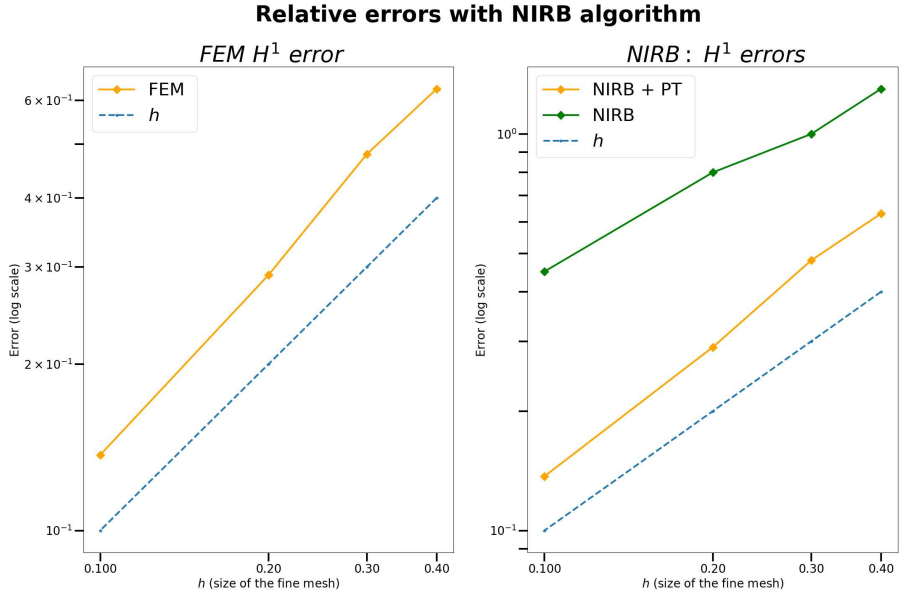

Figure 1: Convergence rate

where the rectification matrix R is a 3rd-order tensor time-dependent. We took 19 parameters in $\mathcal{G}$ for the RB construction such that $\mu_i = 0.5i$ and thus, we obtain 10×19 snapshots with respect to the time variable. Here follow the results with the NIRB algorithm and the rectification post-treatment for a new parameter $\mu = 1$. There are compared to the fine and coarse FEM projection errors. The exact solution is given by

$$u(t, \mathbf{x}; 1) = 10tx^2(1-x)^2y^2(1-y)^2.$$

We implemented both schemes on FreeFem ++ [16] and computed the NIRB rectified error in the maximum-norm. The H^1 NIRB rectified error is defined by

$$\max_{n=1,\dots,(T-t_0)/\Delta t_F} \frac{\left\| u(t_0 + n\Delta t_F)(\mu) - Ru_{Hh}^{N,n}(\mu) \right\|_{H_0^1(\Omega)}}{\left\| u(t_0 + n\Delta t_F)(\mu) \right\|_{H_0^1(\Omega)}}, \tag{64}$$

and this error is compared to the FEM ones defined as

$$\max_{n=1,\dots,(T-t_0)/\Delta t_F} \frac{\left\| u(t_0 + n\Delta t_F)(\mu) - u_h^n(\mu) \right\|_{H_0^1(\Omega)}}{\left\| u(t_0 + n\Delta t_F)(\mu) \right\|_{H_0^1(\Omega)}} \text{ and } \max_{n=1,\dots,(T-t_0)/\Delta t_G} \frac{\left\| u(t_0 + n\Delta t_G)(\mu) - u_H^n(\mu) \right\|_{H_0^1(\Omega)}}{\left\| u(t_0 + n\Delta t_G)(\mu) \right\|_{H_0^1(\Omega)}}. \tag{65}$$

Since both schemes are stable, we can take $\Delta t_F \simeq h$ and $\Delta t_G \simeq H$. In Figure 1, we display the convergence rate of the fine approximations (left) and of the NIRB approximations (with and without rectification). For all meshes, $h \simeq \Delta t_F$, $N = 10, \mu = 1$ and as expected, we observe that both NIRB errors converge in $\mathcal{O}(h + \Delta t_F)$, and that we retrieve the fine error with the rectified solution.

For the Crank-Nicholson scheme we fixed $\Delta t_G = 0.2$ and $H = \frac{\sqrt{2}}{6}$, whereas for the Euler scheme we set $\Delta t_F = 0.1$ and $h = \frac{\sqrt{2}}{12}$. In Figure 2, we plot the errors ((64) with the H_0^1-norm) as a function of the number of modes N between $t_0 = 1$ and $T = 2$ and we compare these results with the FEM errors (65). The NIRB errors saturate very short of reaching the fine errors. In Figure 4, we display the NIRB approximation at several time steps. In 1, we present the maximum H^1-error of the NIRB rectified approximation over the parameters. The error is given by

$$\max_{\mu \in \mathcal{G}_{Ntrain}, n=1,\dots,(T-t_0)/\Delta t_F} \frac{\left\| u_h(t_0 + n\Delta t_F)(\mu) - Ru_{Hh}^{N,n}(\mu) \right\|_{H_0^1(\Omega)}}{\left\| u_h(t_0 + n\Delta t_F)(\mu) \right\|_{H_0^1(\Omega)}}. \tag{66}$$

and the maximum is retrieved for $\mu = 10$.

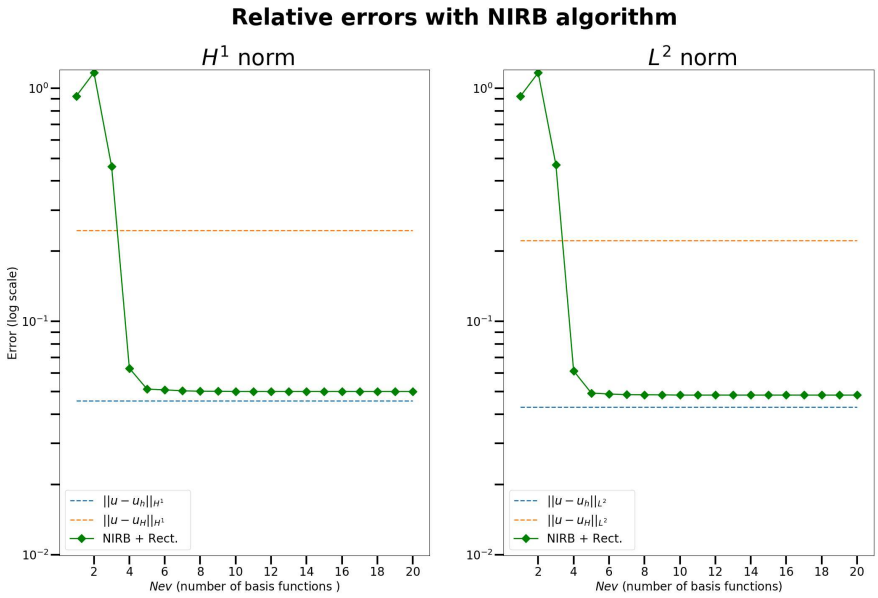

Figure 2: NIRB $L^\infty(0,T;H^1(\Omega))$ (left) and $L^\infty(0,T;L^2(\Omega))$ (right) relative errors with parabolic equations with a new parameter $\mu = 1$

Table 1: Maximum H^1 error over the parameters [$\mu = 10$] (66) (compared to the true NIRB projection and to the FEM coarse projection) with $N = 20$

NIRB rectified error	$\max_{n=1,\dots,(T-t_0)/\Delta t_F} \frac{\left\|u_h(t_0+n\Delta t_F)(\mu) - u_{hh}^{N,n}(\mu)\right\|_{H_0^1(\Omega)}}{\left\|u_h(t_0+n\Delta t_F)(\mu)\right\|_{H_0^1(\Omega)}}$	$\max_{n=1,\dots,(T-t_0)/\Delta t_F} \frac{\left\|u_h(t_0+n\Delta t_F)(\mu) - u_H(t_0+n\Delta t_F)(\mu)\right\|_{H_0^1(\Omega)}}{\left\|u_h(t_0+n\Delta t_F)(\mu)\right\|_{H_0^1(\Omega)}}$
0.05935057678446814	$2.3127816652661065 \times 10^{-10}$	6.844346431223195

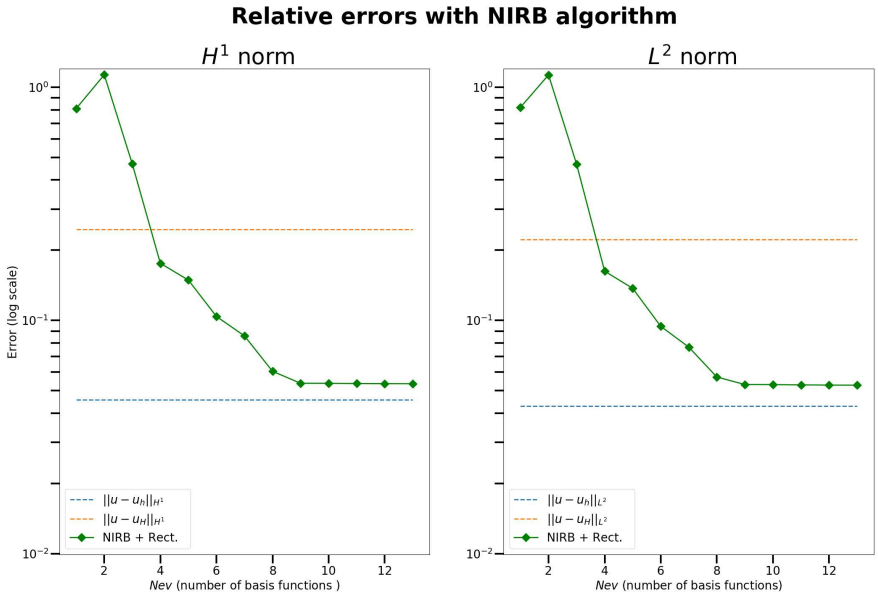

Figure 3: NIRB $L^\infty(0,T;H^1(\Omega))$ (left) and $L^\infty(0,T;L^2(\Omega))$ (right) relative errors with parabolic equations with a new parameter $\mu = 1$, another NIRB decomposition

Remark 5.1. *We may also consider NIRB aproximations of* (14) *under the form*

$$u_{Hh}^{N,n}(\boldsymbol{x};\mu) = \sum_{i=1}^{N} \alpha_i^H(\mu,t^n)\ \Phi_{h,i}^n(\boldsymbol{x}),\ n \geq 0, \tag{67}$$

with $(\Phi_{h,i}^n)_{i=1,\ldots,N}$ *time-dependent basis functions. This time, the greedy algorithm is executed for each time step.*
With this decomposition, we obtained the following results (see Figure 3).

Remark 5.2. *We retrieve the fine and coarse solutions in the VTK format and use Python to execute the NIRB algorithm. For the interpolation in time and in space, we employed linear interpolations (see for instance the Python module "interpolate" with the function "griddata" for space and "interp1d" for the time interpolation).*

5.1.1 Time execution (min,sec)

We present the FEM and NIRB runtimes in 2 and 3.

Table 2: FEM runtimes

FEM high fidelity solver	FEM coarse solution
00:03	00:02

Table 3: NIRB runtimes ($N = 18$)

NIRB Offline	classical rectified NIRB online
1:45	00:02

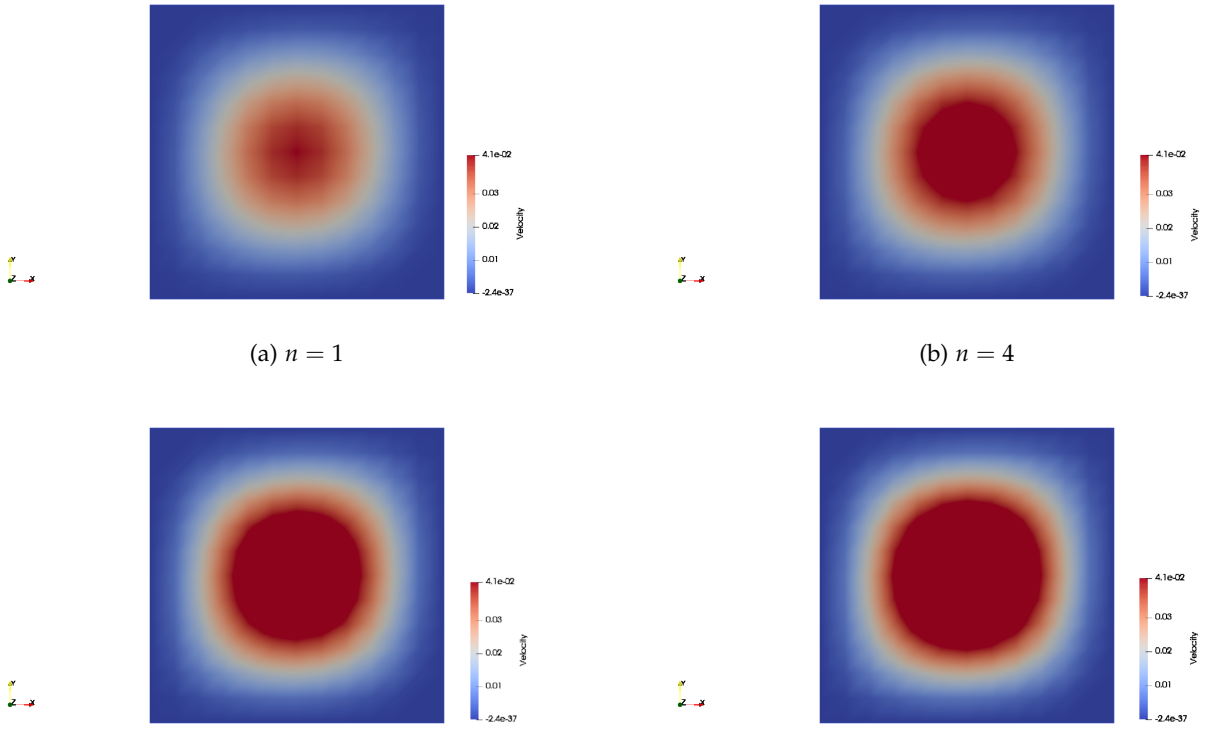

(a) $n = 1$ (b) $n = 4$

(c) $n = 7$ (d) $n = 10$

Figure 4: Evolution of the NIRB approximation for $N = 10$, at time $t = t_0 + n\Delta t_F$, $n = 1, 4, 7$ and 10

5.2 $\Delta t_G^2 = \Delta t_F$

We tried with $H^2 \simeq h \simeq \Delta t_G^2 \simeq \Delta t_F$. As previously, in Figure 5, we display the convergence rate of the fine approximations (left) and of the NIRB approximations (with and without rectification). For all meshes, $h \simeq \Delta t_F$, $N = 10, \mu = 1$ and as expected, we observe that both NIRB errors converge in $\mathcal{O}(h + \Delta t_F)$, and that we retrieve the fine error with the rectified solution. For our tests, we took 10 training parameters $0.5 + i\ 0.5, i = 0, \dots, 9$.

5.3 Brusselator equations

We consider a last test, which consists of the simulation of the Brusselator equation

$$\partial_t u = a + uv^2 - (b+1)u + \boldsymbol{\alpha}\Delta u$$
$$\partial_t v = bu - uv^2 + \boldsymbol{\alpha}\Delta v.$$

Now, we have to deal with a non-linearity, and two unknowns. Our parameter belongs to $\mathbb{R}^3$, $\boldsymbol{\mu} = (a, b, \boldsymbol{\alpha})$. We test our NIRB algorithm on stable solutions and an example with $a = 2,\ b = 4$ is given in Figure 6.

NIRB rectified error	$\max_{n=1,\dots,T/\Delta t_F} \frac{\left\|u_h(n\Delta t_F)(\mu) - u_{hh}^{N,n}(\mu)\right\|_{H_0^1}}{\left\|u_h(n\Delta t_F)(\mu)\right\|_{H_0^1}}$	$\max_{n=1,\dots,T/\Delta t_F} \frac{\left\|u_h(n\Delta t_F)(\mu) - u_H(n\Delta t_F)(\mu)\right\|_{H_0^1}}{\left\|u_h(n\Delta t_F)(\mu)\right\|_{H_0^1}}$
0.5	1.3×10^{-9}	4.5

Table 4: Maximum H^1 error over the parameters [$\mu = 10$] (compared to the true NIRB projection and to the FEM coarse projection) with $N = 20$

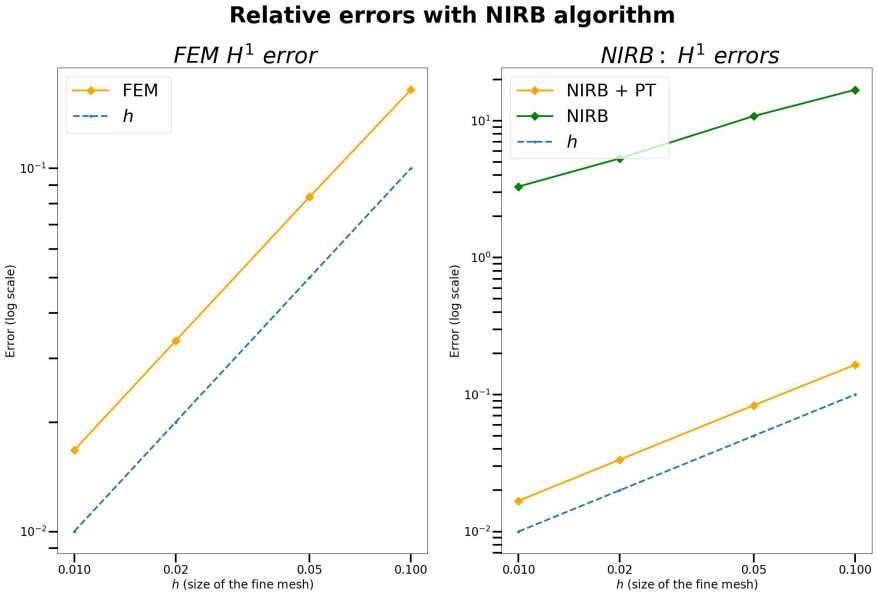

Figure 5: Convergence rate

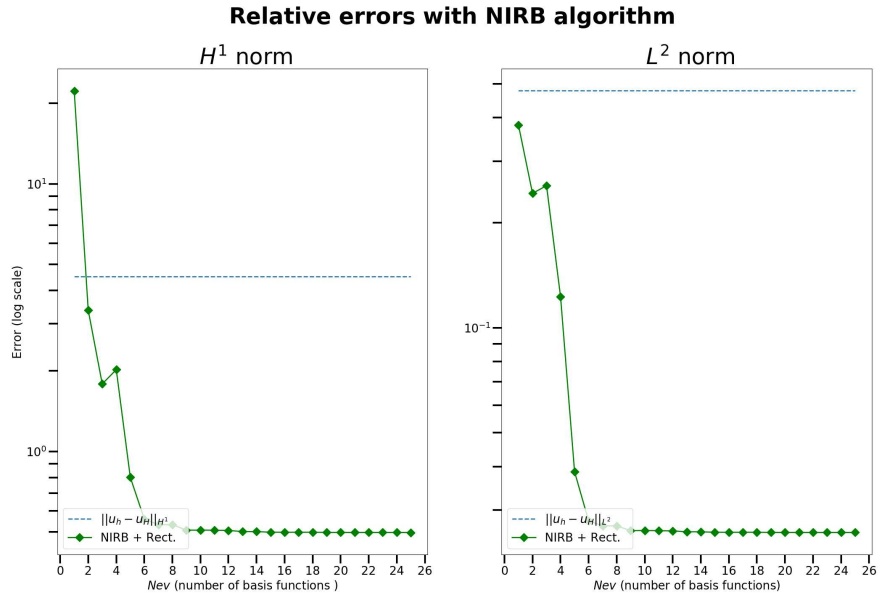

Figure 6: Test with $L^\infty(0,T;H^1(\Omega))$ (left) and $L^\infty(0,T;L^2(\Omega))$ (right) relative errors with a new parameter $\mu = 1$, $T = 2$, $\Omega = [0,1] \times [0,1]$

6 Estimates on the rectification

As observed in our numerical results, the rectification post-treatment allows us to retrieve the error of the fine solutions. This section aims to understand how it works and takes its inspiration from a previous work [21]. We refer to chapter 7 of [21] for the notations.

In the elliptic context, the rectification matrix is defined by (3), whereas in the parabolic context, it is given by algorithm 3, where a loop in time takes place. Thus, for each time step, the rectification post-treatment works as in the elliptic framework, hence we will stick to the unique notation without the time indices.

In both cases, we deal with three linear operators:

- $\pi_N : V_h \to X_h^N$, which represents our fine solutions.
- $\mathcal{I}_N : V_H \subset V_h \to X_h^N$, which is our coarse solutions.
- $\tilde{\pi}_N : V_H \subset V_h \to X_h^N$, which is our rectification operator, which goes from coarse to fine coefficients.

Notation:
u_{hh}^N: true approximation, u_{Hh}^N: NIRB approximation, Ru_{Hh}^N : Rectified NIRB approximation.

By definition,

$$Ru_{Hh}^N(\mu_k) = u_{hh}^N(\mu_k), \forall k = 1, \dots, N. \tag{68}$$

For $k = 1, \dots, N$,

$$\begin{aligned}
\left\| \sum_{i=1}^N (u_h(\mu), \Phi_i^h)\Phi_i^h - \sum_{i,j=1}^N R_{i,j}(u_H(\mu), \Phi_j^h)\Phi_i^h \right\|_{H^1(\Omega)} &\leq \left\| \sum_{i=1}^N (u_h(\mu) - u_h(\mu_k), \Phi_i^h)\Phi_i^h - \sum_{i,j=1}^N R_{i,j}(u_H(\mu) - u_H(\mu_k), \Phi_j^h)\Phi_i^h \right\|_{H^1(\Omega)}, \\
&\leq \sqrt{\lambda_N} \left\| u_h(\mu) - u_h(\mu_k) \right\|_{L^2(\Omega)} + \left\| \sum_{i,j=1}^N R_{i,j}(u_H(\mu) - u_H(\mu_k), \Phi_j)\Phi_i \right\|_{H^1(\Omega)}, \\
&\leq \sqrt{\lambda_N} [\left\| u_h(\mu) - u_h(\mu_k) \right\|_{L^2(\Omega)} + \|\tilde{\pi}_N\|_2 \left\| u_H(\mu) - u_H(\mu_k) \right\|_{L^2}].
\end{aligned}$$

Since the Kolmogorov width is small,

$$E(\mathcal{M}_h, X_h^N) = \sup_{x \in \mathcal{M}_h} \left(\inf_{y \in X_h^N} \|x - y\| \right) \tag{69}$$

is small and thus,

$$\inf \left\| u_h(\mu) - \Phi_h(\mu_k) \right\| \leq E(\mathcal{M}_h, X_h^N) \tag{70}$$

is small too. Now, $\left\| u_H(\mu) - u_H(\mu_k) \right\|_{L^2}$ must be small, so the Kolmogorov width of the coarse solutions needs to be relatively small too. We may numerically prove in our problem model that $\|\tilde{\pi}_N\|_2$ is in $\mathcal{O}(1)$.

References

[1] G. Akrivis, C. Makridakis, and R. Nochetto. A posteriori error estimates for the crank–nicolson method for parabolic equations. *Mathematics of computation*, 75(254):511–531, 2006.

[2] M. Barrault, C. Nguyen, A. Patera, and Y. Maday. An 'empirical interpolation' method: application to efficient reduced-basis discretization of partial differential equations. *Comptes rendus de l'Académie des sciences. Série I, Mathématique*, 339-9:667–672, 2004.

[3] G. Berkooz, P. Holmes, and J L Lumley. The proper orthogonal decomposition in the analysis of turbulent flows. *Annual review of fluid mechanics*, 25(1):539–575, 1993.

[4] S. Brenner and R. Scott. *The mathematical theory of finite element methods*, volume 15. Springer Science & Business Media, 2007.

[5] F. Casenave, A. Ern, and T. Lelièvre. A nonintrusive reduced basis method applied to aeroacoustic simulations. *Advances in Computational Mathematics*, 41(5):961–986, Jun 2014.

[6] R. Chakir. *Contribution à l'analyse numérique de quelques problèmes en chimie quantique et mécanique*. PhD thesis, 2009. Doctoral dissertation, Université Pierre et Marie Curie-Paris VI.

[7] R. Chakir, P. Joly, Y. Maday, and P. Parnaudeau. A non intrusive reduced basis method: application to computational fluid dynamics. In *3rd European Conference on Computational Optimization*. Germany, 20013, Jul.

[8] R. Chakir and Y. Maday. A two-grid finite-element/reduced basis scheme for the approximation of the solution of parametric dependent p.d.e. In *9e Colloque national en calcul des structures*, 2009.

[9] R. Chakir, Y. Maday, and P. Parnaudeau. A non-intrusive reduced basis approach for parametrized heat transfer problems. *Journal of Computational Physics*, 376:pp.617–633, January 2019.

[10] R. Chakir, B. Streichenberger, and P. Chatellier. A non-intrusive reduced basis method for urban flows simulation. 01 2021.

[11] L. C. Evans. *Partial differential equations*. American Mathematical Society, Providence, R.I., 2010.

[12] E. Grosjean and Y. Maday. Error estimate of the non-intrusive reduced basis method with finite volume schemes. *ESAIM: M2AN*, 55(5):1941–1961, 2021.

[13] B. Haasdonk. Convergence rates of the pod–greedy method. *ESAIM: Mathematical modelling and numerical Analysis*, 47(3):859–873, 2013.

[14] B. Haasdonk and M. Ohlberger. Reduced basis method for finite volume approximations of parametrized linear evolution equations. *ESAIM: Mathematical Modelling and Numerical Analysis-Modélisation Mathématique et Analyse Numérique*, 42(2):277–302, 2008.

[15] J. K. Hammond. *Méthodes des bases réduites pour la modélisation de la qualité de l'air urbaine*. PhD thesis, 2017. Thèse de doctorat. Mathématiques Paris Est 2017.

[16] F. Hecht. New development in freefem++. *Journal of numerical mathematics*, 20(3-4):251–266, 2012.

[17] O. Mula Hernandez. *Some contributions towards the parallel simulation of time dependent neutron transport and the integration of observed data in real time*. PhD thesis, Thèse de doctorat. Université Pierre et Marie Curie-Paris VI., 2014.

[18] H. Herrero, Y. Maday, and F. Pla. Rb (reduced basis) for rb (rayleigh–bénard). *Computer Methods in Applied Mechanics and Engineering*, 261:132–141, 2013.

[19] D J. Knezevic and A T. Patera. A certified reduced basis method for the fokker–planck equation of dilute polymeric fluids: Fene dumbbells in extensional flow. *SIAM Journal on Scientific Computing*, 32(2):793–817, 2010.

[20] A. Kolmogoroff. Über die beste annaherung von funktionen einer gegebenen funktionenklasse. *Annals of Mathematics*, pages 107–110, 1936.

[21] Y. Maday and O. Mula. A generalized empirical interpolation method: application of reduced basis techniques to data assimilation. In *Analysis and numerics of partial differential equations*, pages 221–235. Springer, 2013.

[22] C. Makridakis. Space and time reconstructions in a posteriori analysis of evolution problems. In *ESAIM: Proceedings*, volume 21, pages 31–44. EDP Sciences, 2007.

[23] A. Quarteroni, A. Manzoni, and F. Negri. *Reduced Basis Methods for Partial Differential Equations: an introduction*, volume 92. Springer, 2015.

[24] D. Ryckelynck. A priori hyperreduction method: an adaptive approach. *Journal of computational physics*, 202(1):346–366, 2005.

[25] B. Streichenberger. *Approches multi-fidélités pour la simulation rapide d'écoulements d'air en milieu urbain*. PhD thesis, 2021. Thèse de doctorat, Université Gustave Eiffel.

[26] V. Thomée. *Galerkin finite element methods for parabolic problems*, volume 25. Springer Science & Business Media, 2007.